· Original article ·

Genome-wide investigation of lncRNAs for dry eye disease in a desiccating stress mouse model

Xing Yi, Zhu Lijuan, Li Xinyu

引用:行怡,朱丽娟,李新玉. 干燥应激小鼠干眼模型中 lncRNAs 的全基因组研究. 国际眼科杂志, 2026,26(12):2066-2075.

Foundation item: Henan Provincial Medical Science and Technology Research Project (No.LHGJ20210305)
Department of Ophthalmology, the First Affiliated Hospital of Zhengzhou University, Zhengzhou 450000, Henan Province, China

Correspondence to: Yi Xing. Department of Ophthalmology, the First Affiliated Hospital of Zhengzhou University, Zhengzhou 450000, Henan Province, China. yixing8608@163.com
Received: 2025-11-24 Accepted: 2026-06-24

干燥应激小鼠干眼模型中 lncRNAs 的全基因组研究

行 怡,朱丽娟,李新玉

基金项目:河南省医学科技攻关计划联合共建项目(No.LHGJ20210305)
作者单位:(450000)中国河南省郑州市,郑州大学第一附属医院眼科
作者简介:行怡,毕业于华中科技大学同济医学院,博士,副主任医师,研究方向:眼表疾病。
通讯作者:行怡. yixing8608@163.com

摘要

目的:探讨干燥应激诱导的小鼠干眼模型中长链非编码 RNA(lncRNA)的全基因组表达谱。

方法:采用东莨菪碱单独处理[正常对照组(N)]或东莨菪碱联合智能环境控制系统处理[模型组(T)]的方式构建小鼠干眼病模型。提取角膜上皮样本进行全转录组测序及生物信息学分析。通过顺式和反式调控分析,系统研究了 lncRNA 的差异表达谱及其对靶基因表达的调控作用,并利用功能富集分析探讨其潜在生物学功能。

结果:与干眼(DED)的发病机制一致,512 个上调和 201 个下调的差异表达基因显著富集于炎症相关通路。LncRNA 分析在 T 组样本中鉴定出 50 个上调和 38 个下调的差异表达 lncRNA。反式调控分析显示,与差异表达 lncRNAs 共表达的趋化因子相关基因呈上调趋势,而胶原相关基因则呈下调趋势。所鉴定的 lncRNAs 在 T 组样本中均表现出较高的表达水平,其中包括与炎症反应密切相关的 Mirt2。顺式调控分析检测到 5 个上调的 lncRNAs 能够调控其邻近的 6 个 mRNA。这些 mRNA 在 T 组样本中同样高表达,进一步证实了上调 lncRNAs 的潜在重要作用。

结论:本研究突显了 lncRNA 在 DED 发病机制中的异常表达谱及其潜在的调控作用。所鉴定的差异表达 lncRNAs 不仅可作为调节因子影响炎症相关基因的表达,还有望成为 DED 治疗的潜在靶点。

关键词:干眼;RNA 测序;基因表达;长链非编码 RNA(lncRNA);炎症

Abstract

• AIM: To reveal the whole genome of long noncoding RNAs (lncRNAs) in a mouse dry eye disease (DED) model induced by desiccating stress.

• METHODS: DED mouse models were constructed using either scopolamine [normal samples (N)] or scopolamine combined with an intelligently controlled environmental system [treated samples (T)]. The corneal epithelial samples were extracted for whole transcriptome sequencing (RNA-sequencing) and bioinformatic analysis. By regulating target gene expression, the dysregulated expression profiles of lncRNAs were systematically investigated through trans- and cis-regulatory analysis, and their potential functions were explored using functional enrichment analysis.

• RESULTS: Consistent with the pathogenesis of DED, 512 upregulated differentially expressed genes (DEGs) and 201 downregulated DEGs were enriched in inflammatory pathways. LncRNA analysis identified 50 upregulated and 38 downregulated differentially expressed (DE) lncRNAs in the T samples. Trans-regulatory analysis revealed that chemokine-associated genes that co-expressed with DE lncRNAs were upregulated, while collagen-related genes were downregulated. The identified lncRNAs showed consistently higher expression levels in the T samples, including Mirt2, which is associated with inflammatory response. Cis-regulatory analysis detected five upregulated lncRNAs that could modulate six adjacent mRNAs. These mRNAs were more highly expressed in the T samples, demonstrating the potential important roles of upregulated lncRNAs.

• CONCLUSION: This study highlights the dysregulated profile of lncRNAs and their potential regulatory roles in the pathogenesis of DED. The identified DE lncRNAs can serve as regulators influencing the expression of genes involved in inflammation and potential therapeutic targets for DED treatment.

• KEYWORDS: dry eye disease; RNA-sequencing; gene expression; long non-coding RNA (lncRNA); inflammation

DOI:10.3980/j.issn.1672-5123.2026.12.02

Citation: Xing Y, Zhu LJ, Li XY. Genome-wide investigation of lncRNAs for dry eye disease in a desiccating stress mouse model. Guoji Yanke Zazhi(Int Eye Sci), 2026,26(12):2066-2075.

INTRODUCTION

Dry eye disease (DED) is a common eye disease observed at ophthalmology clinics, with an incidence ranging from 4.7% to 62.9%[1]. Various factors, reasons such as aqueous deficiency and strong tear evaporation, lead to the creation of unstable and hypertonic tear film, triggering an inflammatory cycle on the ocular surface and epithelial damage. These factors mutually reinforce the transformation of DED into a chronic, permanent disease characterized by symptoms such as eye discomfort and blurred vision affecting work and life[1]. Several factors, such as dry environmental conditions, induce corneal epithelial cell (CEC) events involving tumor necrosis factor-α (TNF-α)/matrix metalloproteinases (MMP) pathway and the cyclic GMP-AMP synthase-stimulator of interferon genes pathway[2-3]. These responses are associated with the increased production of inflammatory cytokines, such as interleukin (IL)-12a, IL-1β, IL-18, and TNF-α, as well as chemokine genes such as C-C chemokine ligand (CCL)-2[4-5]. The CECs activate and recruit inflammatory cells, such as T helper 1 cells, which release interferon-γ on to the ocular surface, where it acts as an additional inflammatory mediator[1]. Inflammatory mediators and tear hyperosmolar pressure lead to the loss of CECs[6] and goblet cells, amplifying or initiating ocular surface hyperosmolality, thereby completing a vicious circle promoting DED from the compensatory phase to the perpetuation stage.

Anti-inflammatory drugs currently in clinical use are used to treat inflammatory responses at different stages of DED. Corticosteroid eye drops provide rapid relief of acute symptoms and prevent damage to the ocular surface by inhibiting MMP-9, inflammatory factors, and inflammatory cells. However, long-term use of corticosteroids is associated with the risk of cataract formation and glaucoma, limiting their clinical application in the treatment of chronic ocular surface inflammation in DED[7-8]. At present, clinically approved drugs for the treatment of chronic inflammation in DED are cyclosporine and lifitegrast. Although both drugs can inhibit T cell activation and inflammatory factor production, neither can address the activation of inflammatory mediators and mitogen-activated protein kinase (MAPK) stress signaling pathways to effectively treat the acute damage caused by dryness to the ocular surface and relieve discomfort[9-11]. Biomolecular therapies such as lacritin, a glycoprotein, have been studied in animal models, but their clinical efficacy needs further confirmation by clinical studies[12]. The current aim in DED treatment is the development of drugs that can address both acute and chronic ocular surface inflammatory reactions without serious side effects. In meeting this aim, gene molecules are receiving increasing attention as novel targets.

Abnormalities in the regulation of long non-coding RNA (lncRNA), a modular molecule with independent domains, exist in many complex human diseases[13]. LncRNAs can specifically bind to DNA, RNA, and proteins to regulate the expression of locally coded protein genes at the levels of chromatin remodeling, transcriptional control, and post-transcriptional processing[13]. Current studies into the expression profile of lncRNAs for DED have been conducted in the corneal or conjunctival tissue of mouse models[14-15]. Although damage and cellular alterations in the CECs play important roles in the pathological process of DED, the molecular mechanism underlying the role of lncRNAs in the CECs of DED remains unclear. To clarify their role, we conducted whole transcriptome sequencing [RNA-sequencing (RNA-seq)] experiments and bioinformatics analysis of the CECs of mice injected with scopolamine combined with an intelligently controlled environmental system (ICES) to systematically investigate the dysregulated expression profile of lncRNAs, and explored their potential functions by regulating the expression of target genes.

MATERIALS AND METHODS

Ethical Approval All protocols complied with the Society for Vision and Ophthalmology Statement on Animal Use, and all animals were modeled according to the guidelines of the Ethics Committee of Zhengzhou University (Ethics Code: 2025-KY-1323-001).

Dry Eye Disease Mouse Model Twelve 7-week-old specific pathogen-free Balb/c mice (24 eyes) were randomly divided into the normal group ($n=6$) and the treated group ($n=6$) and provided with adequate food and water. Scopolamine solution (0.5 mg/0.2 mL) was injected alternately into the left and right hind limbs of both groups four times a day (at 8 a.m., 11 a.m., 2 p.m., and 5 p.m.) for 4 d. The treated group was housed in an environment of 0% humidity at a temperature ranging from 21℃ to 23℃. For 1 h, three times a day for a total of 4 d, the treated group was placed on an ultra-clean table at the maximum airflow rate. The normal group was housed in an environment of 50%-80% with no airflow at a temperature ranging from 21℃ to 23℃. Schirmer's I test score and corneal fluorescein sodium staining photos were recorded before treatment and on day 5 post-treatment.

Detection of Basal Tear Secretions (Schirmer's I-test) Schirmer's I-test was performed using the phenol red thread tear test with a Tianjin Jingming Phenol-Red cotton thread (Tianjin, China). After intraperitoneal injection of 1.25% avertin (0.2 mL/10 g) under general anesthesia, the folded end of the phenol red cotton thread was inserted 1 mm into the lower lateral conjunctival vault of the right eye for 30 s. The color of phenolic cotton changes from yellow to red with the secretion of tears. The wetting length (mm) of the band indicated by the red dye was read and recorded, and the measurement was repeated three times in each eye to take the average. The mice were assisted in closing their eyes after examination.

Corneal Fluorescein Sodium Staining Corneal fluorescein staining was evaluated in the left eye. After injection of 50 μL of 5% fluorescein sodium solution (Sigma 46960-25G-F; Sigma-Aldrich, St. Louis, MO, USA) into the inferior conjunctival sac with a micropipette, corneal fluorescence staining was examined by slit lamp microscopy with the cobalt

blue light illuminated. Photographs were taken through a slit lamp with cobalt blue light illumination.

Sample Collection After mice were euthanized using excessive isoflurane inhalation (Lunan Pharmaceutical, Shandong, China), one eye from each group was collected for histological evaluation. Each eyeball and eyelid were fixed in 10% formalin, dehydrated, embedded in paraffin, cross-sectioned, and stained with periodic acid-Schiff reagent. All remaining animals (n = 10) were sampled, and after tissue harvesting, the eyeballs were rinsed with pre-cooled phosphate-buffered solution three times. CECs were gently scraped under a microscope (Mshot MF53, Mingmei, Guangzhou, China) using a blade until the Bowman's membrane (identified by its smooth surface) was exposed across of the entire cornea. CECs samples from both eyes of each mouse were placed in a 1.5-mL centrifuge tube label with the sample name and serial number, then rapidly cryopreserved with liquid nitrogen.

RNA Extraction and RNA-Seq Total RNA was treated with RQ1 DNase (Promega, Fitchburg, WI, USA) to remove DNA. The quality and quantity of the purified RNA were determined by measuring the absorbance at 260 nm/280 nm (A260/A280) using Nanodrop One (Thermo Fisher Scientific, Waltham, MA, USA). RNA integrity was further verified by 1.5% agarose gel electrophoresis. For each sample, 1 μg of total RNA was used for RNA-seq library preparation. Ribosomal RNAs were depleted with the Ribo-off™ rRNA depletion kit (Vazyme, Nanjing, USA, N406-01). The purified RNA was employed for directional RNA-seq library preparation using the KAPA Stranded mRNA-Seq Kit for the Illumina® Platform (KK8544; Illumina, San Diego, CA, USA). Polyadenylated mRNAs were purified and fragmented before being converted into double-strand cDNA. Following end repair and A tailing, the DNAs were ligated using a Diluted Roche Adaptor (KK8726; Roche, Basel, Switzerland). Products corresponding to 300-500 bps were selected after purification and ligation. The ligated products were then amplified, purified, quantified, and stored at -80℃ before sequencing. The strand marked with dUTP (the second cDNA strand) was not amplified, allowing strand-specific sequencing. For high-throughput sequencing, the libraries were prepared following the manufacturer's instructions, and the Illumina Novaseq 6000 system was used for 150 nt paired-end sequencing.

RNA-Seq Raw Data Cleaning and Alignment After raw reads containing more than 2-N bases were discarded, adaptors and low-quality bases were trimmed from raw sequencing reads using the FASTX-Toolkit (Version 0.0.13). Short reads less than 16 nt were also discarded, and then clean reads were aligned to the mouse GRCm39 genome by HISAT2[16], allowing no more than four mismatches. Uniquely mapped reads were used for gene read number counting and calculation of fragments per kilobase of transcript per million fragments mapped (FPKM)[17].

Differentially Expressed Gene Analysis The R Bioconductor package DESeq2[18] was utilized to screen out differentially expressed genes (DEGs). P<0.05 and fold change >1.5 or < 0.67 were set as the cut-off criteria for identifying DEGs.

Assembly of Predicted Transcripts After the RNASeq were grouped, StringTie2[19] was used to assemble the data of each group and predict the transcripts. The expression of the predicted transcripts of each group was screened, the transcripts with FPKM<1 were eliminated, and StringTie2 was used to combine the remaining transcripts into one transcript (a GTF file).

LncRNA Prediction To predict credible lncRNAs, four analysis software packages—CPC2[20], LGC[21], CNCI[22] and CPAT[23]—were used to predict lncRNAs. The noncoding transcripts identified by the four software packages were counted. Transcripts that overlapped with the known coding genes, were less than 200 bp in length, had potential coding ability, and were less than 1000 bp away from the nearest gene from the assembly results were successively removed. The prediction results of the new lncRNAs were obtained using four software tools, and only the lncRNAs identified by all four software packages (the intersection set) were retained for subsequent analysis and processing.

LncRNA Cis-Regulatory Target The threshold of co-location was set as 100kb upstream and downstream of lncRNA in the trans-regulatory relationship pair[24]. The Pearson's correlation coefficient (PCC) between the lncRNA and their neighboring mRNAs was then calculated to evaluate co-location relationships. LncRNA-mRNA with an absolute PCC > 0.8 and P < 0.01 were considered potential cis-regulatory target pairs. The intersection of the co-location and co-expression datasets was determined to obtain the cis target of lncRNA.

Functional Enrichment Analysis To determine the functional categories of DEGs, Gene Ontology terms and Kyoto Encyclopedia of Genes and Genomes (KEGG) pathways were identified using the KOBAS 2.0 server[25]. Hyper-geometric testing and the Benjamini-Hochberg false discovery rate controlling procedure were used to define the enrichment of each term.

Availability of Data and Materials The data supporting the findings of this study can be obtained from the corresponding author upon reasonable request.

RESULTS

Mouse Model of DED After 4 d of treatment with scopolamine or scopolamine combined with ICES, fluorescent sodium dye revealed significant epithelial punctate defects in the treated group compared with the normal group. No difference in fluorescence was observed between the two groups by slit lamp examination before treatment (day 0) (Figure 1A). A thinner epithelium and more severe atrophy of conjunctival goblet cells were observed in the treated group (Figure 1B). Both groups had similar tear production before treatment. After treatment, tear production in the treated

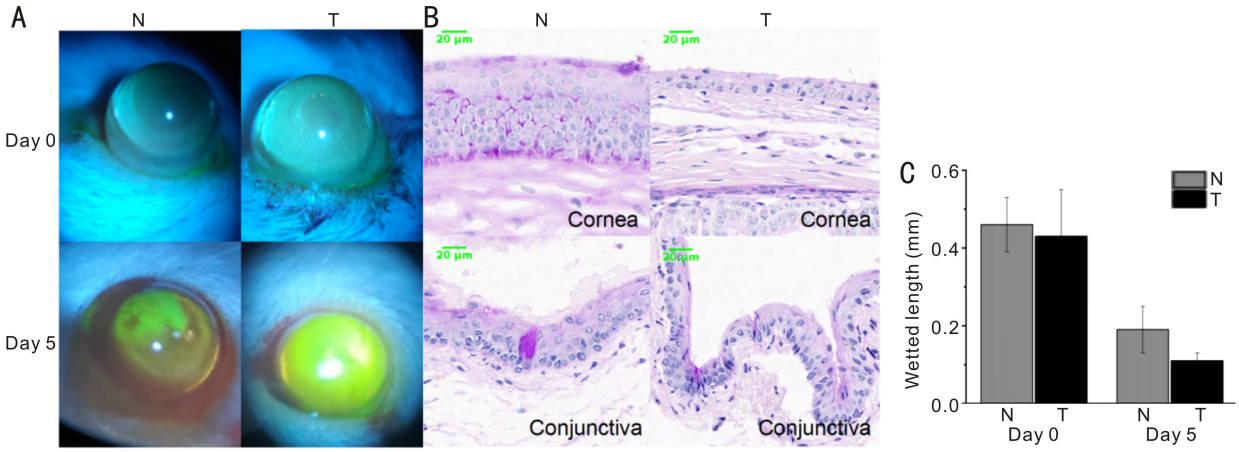


Figure 1 Identification of long noncoding RNAs in the eye tissue of mice A: Fluorescent sodium staining of the cornea in the T and N groups on days 0 and 5; B: Cornea and conjunctiva periodic acid-Schiff staining in the T and N group on day 5; C: Compared with that on day 0, the wetted length of the phenol red cotton thread on day 5 was significantly reduced. On day 5, the wetted length was significantly smaller in the T group than in the N group ($P<0.05$). DED: Dry eye disease. Error bars represent mean±standard error of the mean.

group decreased rapidly and significantly compared with the normal group (0.19 ± 0.06 *vs* 0.11 ± 0.02, respectively, $P<0.05$, Figure 1C).

Dysregulated Transcriptome Profile in CECs of DED Mice After successful construction of the DED mouse model, CECs from treated and normal mice were extracted to perform whole transcriptome RNA-seq experiments. The outlier N3 sample was excluded, and five treated samples (T) and four normal samples (N) were prepared as biological replicates. After aligning quality-filtered reads onto the mouse GRCm39 genome using HISAT2 software[16], the expression levels of all detected genes were calculated. The principal component analysis (PCA) results demonstrated that the T and N samples were clearly separated based on the total expressed genes, suggesting that the global transcriptome profile of the T samples had significantly changed compared with the N samples. DEG analysis to identify the dysregulated genes in the T and N samples revealed 512 upregulated DEGs and 201 downregulated DEGs in the T samples, implying that scopolamine and blowing treatment could induce more upregulated genes in mouse CECs. Functional enrichment analysis of upregulated and downregulated DEGs showed that they were enriched in distinct pathways. Upregulated DEGs were enriched in visual perception, inflammatory response, and chemotaxis-associated pathways, while downregulated DEGs were enriched in extracellular matrix organization, response to drugs, several metabolic process pathways, and cellular process pathways. Some of these enriched pathways, including inflammatory response- and chemotaxis-related pathways, are associated with the pathogenesis of DED[26]. These results together demonstrate that genes associated with DED are dysregulated at the RNA expression level in the T samples.

Genome-Wide Identification and Profile of LncRNAs in CECs of DED Mice As regulatory molecules, lncRNAs are differentially expressed in CECs and play important roles in the pathogenesis of ophthalmological disorders[27]. Therefore, the lncRNA expression profile in T and N samples was systematically investigated. Initially, novel transcripts were predicted and their coding potential calculated to select novel lncRNAs. Comparison of known and novel lncRNAs identified 10 times more known lncRNAs than novel lncRNAs, and the T and N samples exhibited almost the same detection levels. The T and N groups shared most of the identified lncRNAs, with 4847 overlapping transcripts detected in both groups (Figure 2A). Analysis of the exon numbers of mRNAs, known lncRNAs, and novel lncRNAs revealed that most lncRNAs, especially novel lncRNAs, had fewer than five exons. Analysis of the length of these three RNA types showed that lncRNAs, especially novel lncRNAs, were much shorter compared with mRNAs. The results of this feature analysis are consistent with the known features of lncRNAs[26]. The PCA results for all detected lncRNAs exhibited a similar pattern to all detected genes, showing obvious inter-group differences (Figure 2B).

Differentially expressed lncRNA (DE lncRNA) analysis revealed much fewer DE lncRNAs compared with DEGs, including 50 upregulated DE lncRNAs and 38 downregulated DE lncRNAs (Figure 2C). Individual difference observed among the T and N samples and the DE lncRNAs are shown in the hierarchical clustering heatmap of DE lncRNAs (Figure 2D). Regarding upregulated DE lncRNAs in T samples, most had the highest levels in the T1 sample. Regarding downregulated DE lncRNAs, most showed better consistency between the N and T samples compared with the upregulated DE lncRNAs (Figure 2D). When the DE lncRNAs of the T and N samples were compared, several host genes of miRNAs, including Mir124a-2hg, the host gene of miR-124a (Figure 2E), were observed. One known lncRNA, Mirt2, which has a protective role in the aberrant activation of inflammation[28], was more highly expressed in the T samples (Figure 2E). The upregulation of Mirt2 in DED

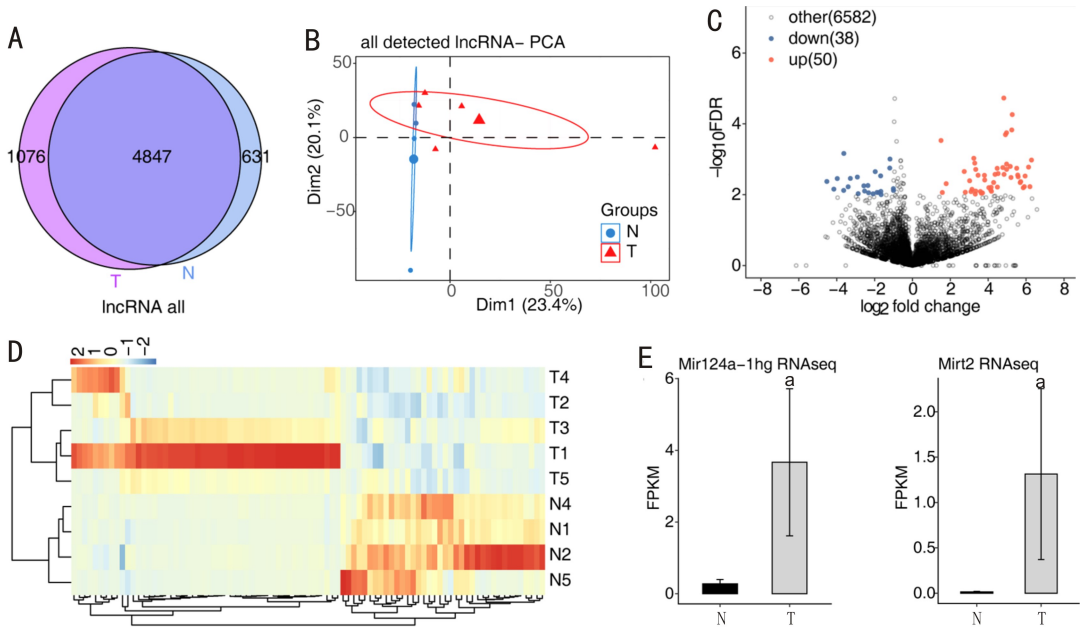


Figure 2 Identification of long noncoding RNAs (lncRNAs) in the eye tissue of mice A: Venn diagram showing the overlapped numbers of all detected lncRNAs. The known and new predicted lncRNAs were combined; B: Principal component analysis based on fragments per kilobase of transcript per million fragments mapped value of all detected lncRNAs. The ellipse for each group is the confidence ellipse; C: Volcano plot showing all differentially expressed (DE) lncRNAs using DEseq2. $P<0.05$ and fold change ≥ 1.5 or ≤0.67; D: Heat map showing the expression levels of all DE lncRNAs; E: Bar plot showing the expression pattern and significant difference between two DE lncRNAs. Error bars represent mean±standard error of the mean. $^aP<0.01$.

indicates that Mirt2 may play important roles in the development of DED by modulating inflammation.

Trans-Regulation of Potential DED-Associated Genes by DE LncRNAs As regulatory RNAs, lncRNAs perform their functions in various manners[29]. LncRNAs acting in a trans manner have nonnegligible roles in gene expression regulation and often exhibit correlated expression patterns with their target genes[30]. To investigate the potential functions of DE lncRNAs, expression correlation analysis was performed between DE lncRNAs and DEGs, setting the absolute PCC> 0.8 and $P<0.01$. Not only were a large number of DE lncRNAs found to be correlated with DEGs but the upregulated lncRNAs were also found to be more highly correlated with DEGs compared with the downregulated lncRNAs. Moreover, several upregulated lncRNAs were found to have more highly significant levels and to be more highly correlated with DEGs, including XLOC_003178, Gm4610, F630040K05Rik, A1847159, and XLOC _ 032737 (Figure 3A). The top 10 lncRNAs most highly correlated with DEGs have more than 300 correlated DEGs, including four DE lncRNAs with more than 350 correlated DEGs (Figure 3B). LncRNA Mirt2 was correlated with 365 DEGs, suggesting its potential regulatory role (Figure 3B).

To better illustrate the interaction network between DE lncRNAs and DEGs, network analysis was performed between these two gene sets, and the enriched functions of the correlated DEGs were analyzed. As shown in Figure 3C, a dense correlation network was observed between DE lncRNAs and DEGs. Functional analysis of the correlated DEGs revealed that they were enriched in visual perception, retina development in camera-type eye, detection of light stimulus involved in visual perception, photoreceptor cell maintenance, cellular response to lipopolysaccharide, chemical synaptic transmission, chemotaxis, neutrophil chemotaxis, and inflammatory response (Figure 3C). The enriched pathways were associated with normal ocular functions and DED pathogenesis, suggesting the regulatory roles of DE lncRNAs. When the expression pattern of the top 10 DE lncRNAs correlated with genes from enriched pathways were plotted, all were found to be upregulated in the T samples (Figure 3D), implying that upregulated DE lncRNAs may have important functions in DED. Plotting of the expression pattern of important genes co-expressing with upregulated DE lncRNAs, mainly the upregulation of chemokine-associated genes and the downregulation of collagen-related genes, suggests dysregulated inflammation and extracellular matrix organization in the DED samples (Figure 3E).

Cis-Regulation of Potential DED-Associated Genes by DE LncRNAs Another important regulatory manner in which lncRNAs regulate their gene expression or chromatin structure adjacent to their genomic locus is in a cis manner[29]. Therefore, dysregulated lncRNAs and their adjacent genes were systematically investigated to predict their functional manner. In addition to their positional relationship (<100 kb), the correlation between DE lncRNAs and their adjacent genes was determined using the criteria PCC>0.8 and $P<0.01$. Five lncRNAs —XLOC _ 003178, Siglecl1, Tmem147os, Gm10030, and XLOC_032536 (Figure 4A)— and six mRNAs —Lrrc2, Sh2d5, Cd33, Dmkn, Ifi202b, and Ifi 2 1 1 (Figure 4 B) — were found to be regulated in a cis -

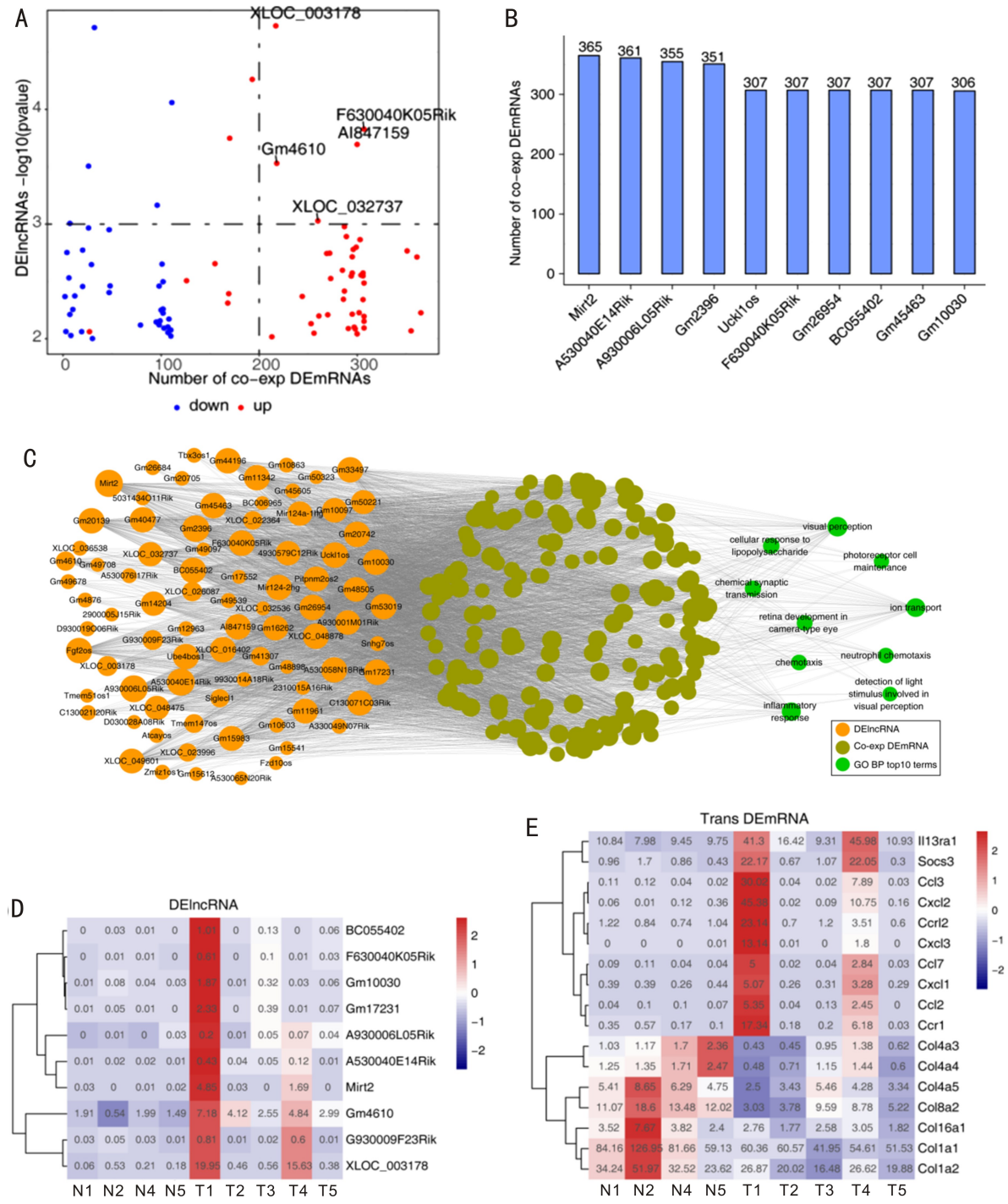


Figure 3 Trans-regulatory genes of differentially expressed long noncoding RNAs (DE lncRNAs) associated with dry eye disease A: Scatter plot showing the correlation analysis results of DE lncRNAs and DE mRNAs. Red points denote upregulated lncRNAs, and blue points denote downregulated lncRNAs. Cutoffs values of $P \leqslant 0.01$ and Pearson's correlation coefficient $\geqslant 0.8$ were applied; B: Bar plot showing 10 DE lncRNAs with the largest number of co-expressed DE mRNAs; C: Network showing the top 10 Gene Ontology biological process enrichment terms of DE mRNAs co-expressed by DE lncRNAs; D, E: Heat map showing the expression profile of DE lncRNAs and co-expressed DE mRNAs.

regulatory manner. Hierarchical clustering heatmap analysis of the five DE lncRNAs and six mRNAs showed that they were all more highly expressed in the T samples. Another finding was that these five DE lncRNAs and six mRNAs showed higher expression levels in T1 and T4 samples (Figure 4A, 4B), revealing their co-expression pattern. Examination of the DE lncRNA-mRNA cis-regulatory pairs revealed that the novel lncRNA-XLOC_003178 formed cis-regulatory pairs with Ifi202b and Ifi211, two mRNAs. Another four pairs were XLOC_032536-Sh2d5, Gm10030-Lrrc2, Siglecl1-Cd33, and Tmem147os-Dmkn (Figure 4C). Read density and expression difference analysis of the T and N samples for two cis-regulatory pairs, namely Gm10030-Lrrc2 and XLOC_003178-Ifi202b/Ifi211, showed higher expression in the T samples (Figure 4D, 4E). These results demonstrate that the identified DE lncRNAs may have a regulatory role in

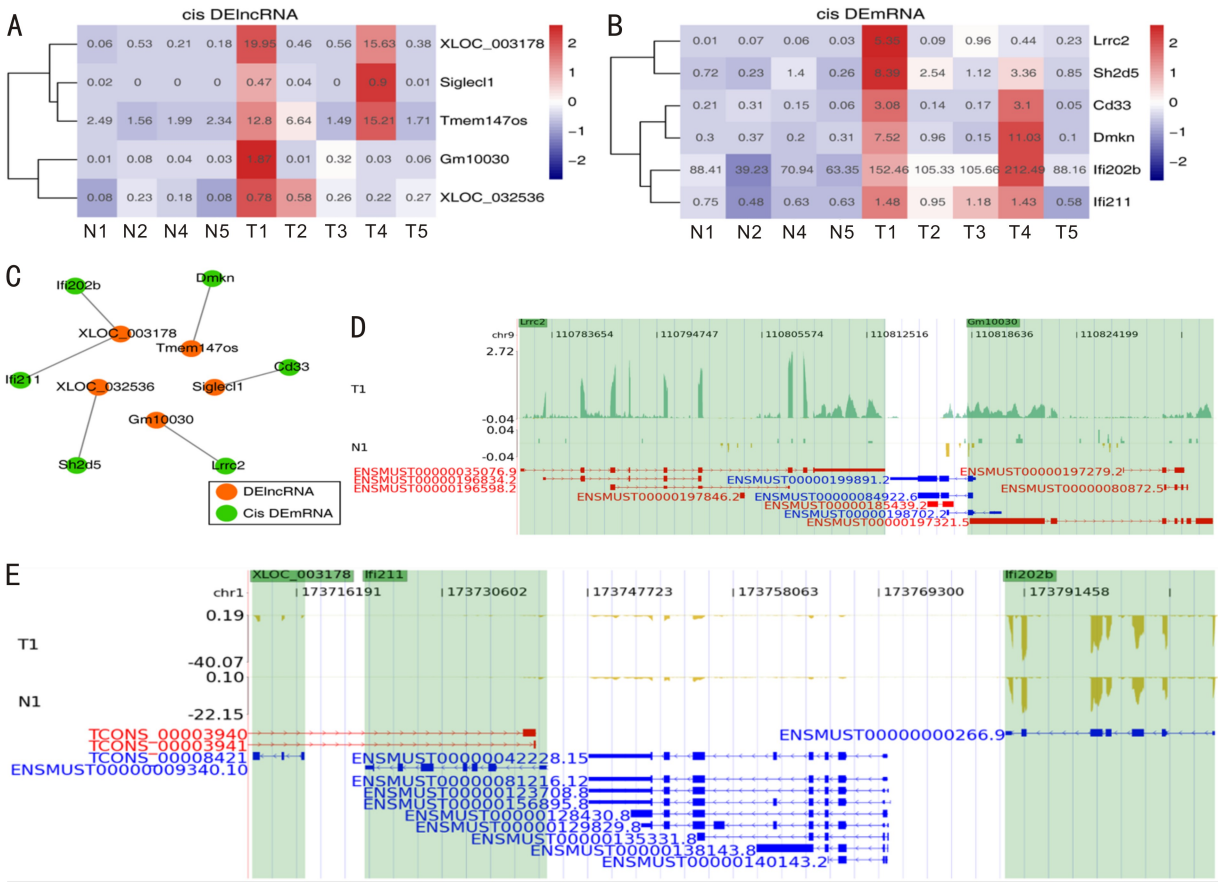


Figure 4 Cis-regulatory genes of differentially expressed long noncoding RNAs (DE lncRNAs) demonstrating the regulatory role of DE lncRNAs A, B: Heat map showing the expression profile of DE lncRNAs and cis mRNAs; C: Network showing DE lncRNAs and paired cis mRNAs; D: Reads cumulative distribution plot showing reads abundance and positional relationship of Gm10030 and Lrrc2; E: Reads cumulative distribution plot showing reads abundance and positional relationship of XLOC_003178, Ifi211, and Ifi202b.

modulating the expression of their adjacent mRNAs.

DISCUSSION

As it is often difficult to obtain ocular surface tissue from DED patients, other specimen types must be used to obtain essential genetic information. When selecting specimens and analyzing results, it is essential to fully consider both microenvironmental differences and species variations. One study that used the RNA-seq results from *in vivo* and *in vitro* samples of human SV40 immortalized CEC lines grown in hypertonic environments and the CECs of desiccating stress (DS) mouse models identified ferroptosis in the enrichment pathways[31]. Another study found that tear film containing miRNAs may be associated with DED inflammatory pathways, but the results showed considerable variability, and the origin of tear miRNAs remains unclear[32].

Various animal models can be used for DED research. Differences in the expression profiles of non-coding genes among species lead to varying sequencing results. Mice have become more common and valuable tool for genetic research due to their more powerful genome databases than rabbits[33]. The unique characteristics of various DED models are crucial in delineating the pathogenesis of different types of DED. The benzalkonium chloride model effectively mimics the manifestations of inflammation and corneal nerve damage[34]. A study that used the corneal tissues of this model revealed that the neuroactive ligand-receptor interaction signaling pathway is particularly affected in DED. The DE lncRNAs Chrnb2 and Gabarapl2 may be involved in the inflammatory response of DED by regulating TNF-α, IL-1β, and IL-6[14]. In a lacrimal gland excision model that simulates persistent tear deficiency[34], single-cell sequencing analysis revealed that S100a9 was significantly upregulated in CECs. The model experienced remission from chronic corneal inflammation after inhibition of S100a9[35].

The DS model is suitable for studying acute inflammation arising from DED. Scopolamine is used to simulate the features of aqueous deficient DED, while ICES is used to produce the features of evaporative DED. In a study using the DS model combined scopolamine with ICES, RNA-seq analysis of CECs identified the ferroptosis pathway[31]. We compared scopolamine with scopolamine combined with ICES, which simulated the differences between aqueous-deficient and mixed DED. A previous study found that scopolamine exerted a significant effect on the nature of inflammatory and ocular surface responses in DED by inhibiting cholinergic activity[36]. Using mice treated with only scopolamine as a control group helped to eliminate this potential interference. We observed that the CEC damage of the combined model was significantly

more severe and that multiple DE lncRNAs were associated with inflammatory, suggesting that lncRNAs may be involved in the acute CEC damage induced by DS through inflammatory pathways.

Multiple ocular surface tissues participate in the pathological process of DED, and different tissues can be selected for research, depending on the specific objectives of a study. One analysis of the RNA-seq profiles of immune cells sorted in conjunctival in DS mice found that DS stimulated different gene expression patterns in conjunctival phagocytocytes[37]. A similar RNA-seq analysis of immune cells from the corneal tissues of DE mice observed increased expression of cytokine and chemokine genes and inflammation markers, as well as decreased expression of complement genes[38]. Another study observed significant changes in KEGG pathways related to apoptosis in the meibomian gland tissue from a diabetes-induced meibomian gland dysfunction mouse model[39].

Our study investigated CECs, which have been reported to exhibit inflammation, and activation of the MAPK and nuclear factor (NF)-κB stress signaling pathways under hyperosmotic conditions[2,5-6]. Among the significantly upregulated DE lncRNA genes that have been associated with inflammation, Mir124-2hg is associated with autophagy and endoplasmic reticulum stress[40]. LncRNA Mirt2 has been shown to act as a negative feedback modulator of excessive inflammation in signaling pathways. For example, Mirt2 is associated with and attenuates ubiquitination of TRAF6's Lys63 ligation, thereby inhibiting the activation of NF-κB and MAPK pathways and limiting the production of pro-inflammatory cytokines[28].

We observed that chemokine-related genes were significantly upregulated in the T samples. Consistent with these observations, previous studies have reported the expression of CCR5 and its ligands were founnd to expressed in the tear film and on the ocular surface in DED patients[41], and the levels of chemokines CCL3/MIP-1α and CCL4/MIP-1β were significantly increased in the tear film of patients with Sjögren's syndrome[42]. In a sample of patients with moderately evaporative DED, IL-8/CXCL8 levels correlated with pain and clinical parameters of moderate evaporative DED[43]. We also found a significant downregulation of genes related to collagen in the T samples. Studies have reported that corneal collagen is susceptible to MMP-induced destruction, digestion, and thinning in DED. Collagen contains binding sites that act as ligands for several inflammatory and immunomodulatory agents. Fragmented collagen not only challenges these receptor-ligand binding relationships but also promotes the recruitment and motility of pro-inflammatory immune cells[44]. Using cis-regulatory analysis, we identified seven lncRNA-mRNA regulatory pairs, including Gm10030-Lrrc2 and XLOC_003178-Ifi202b/Ifi211. Lrrc2 is a member of a family of leucine-rich repeating proteins that play an important role in the inflammatory response as integrators for immune pattern recognition and signaling[45]. Ifi202b and Ifi211 are both interferon-inducible genes. Studies using a depression-related DED mouse model showed a significant increase in interferon-γ protein expression in the cornea[46]. Non-coding RNAs, such as miRNAs and lncRNAs, form complex regulatory networks that play a key role in the post-transcriptional regulation of mRNA expression. MiRNAs act as negative regulators of gene expression through RNA interference mechanisms. In human CECs exposed to hyperosmolar stress, overexpression of miR-16-5p or miR-142-3p significantly reduces oxidative stress and COX-2 expression by inhibiting NF-κB-mediated cytokine expression[47]. Through the downregulation of MAP3K8, miR-93-5p protects CECs from hyperosmolar damage[48]. LncRNA can interact with miRNAs, either binding to the miRNAs themselves or to their targets, preventing miRNA from regulating mRNA. In tears from patients with DED and in human conjunctival epithelial cells, the expression of lncRNA SNHG7 increases, while that of miR-146a-5p decreases. The downregulation of SNHG7 can reduce inflammation levels[49].

This study has several limitations that should be acknowledged. One limitation is that the findings may be limited in terms of generalizability and reliability due to the lack of validation trials. The specific role of lncRNAs in the pathogenesis of DED has not been fully verified, and the potential contributions of other factors or pathways cannot be excluded. Therefore, it may bepremature to attribute causality to lncRNAs alone. Another limitation was the use of only five mice in the treated group and four in the normal group. Our use of small sample sizes may not have provided sufficient statistical power to detect subtle but important differences or generalize the findings to larger populations.

In future research, we will focus on addressing the limitations of this study. We will increase the sample size to improve the stability and reproducibility of the results when we perform genetic validation. The therapeutic efficacy of targeting specific lncRNAs against ICES-induced CEC damage will be assessed following *in vivo* drug intervention using Schirmer's I test and corneal fluorescein staining. Using cell models, we will delve into the role of lncRNAs in DED-related cell signaling pathways, specifically by regulating lncRNA expression and observing its effects on cell function. Using RNA-seq and bioinformatic analysis of CECs from DED mouse models treated with scopolamine or scopolamine combined with ICES, we observed DEGs and DE lncRNA related to inflammation. Based on our findings, we will conduct further verification experiments to elucidate the mechanism by which lncRNAs regulate inflammatory signal pathways, thereby providing a potential approach for preventing the damage of DS on CECs in DED.

Conflicts of Interest: Xing Y, None; Zhu LJ, None; Li XY, None.

Data Availability Statement: The data supporting the findings of this study can be obtained from the corresponding author upon reasonable request.

Authors' Contributions: Xing Y and Li XY performed the *in*

vivo experiments and analyzed the data. Xing Y and Zhu LJ designed and supervised the project, and wrote the manuscript. All authors contributed to manuscript revision, read, and approved the submitted version.

REFERENCES

[1] Stapleton F, Argüeso P, Asbell P, et al. TFOS DEWS III: digest. Am J Ophthalmol, 2025,279:451-553.

[2] Zhang Y, Yang M, Zhao SX, et al. Hyperosmolarity disrupts tight junction *via* TNF-α/MMP pathway in primary human corneal epithelial cells. Int J Ophthalmol, 2022,15(5):683-689.

[3] Tan XY, Chen QQ, Chen ZH, et al. Mitochondrial DNA-activated cGAS-STING signaling in environmental dry eye. Invest Ophthalmol Vis Sci, 2024,65(4):33.

[4] Zibandeh N, Yıldız E, Özer B, et al. Androgen suppresses hyperosmolarity - induced inflammatory mediators in human corneal epithelial cells. Cornea, 2020,39(7):886-891.

[5] Yu ZY, Yazdanpanah G, Alam J, et al. Induction of innate inflammatory pathways in the corneal epithelium in the desiccating stress dry eye model. Invest Ophthalmol Vis Sci, 2023,64(4):8.

[6] Yang X, Zuo X, Zeng H, et al. IFN-γ facilitates corneal epithelial cell pyroptosis through the JAK2/STAT1 pathway in dry eye. Invest Ophthalmol Vis Sci, 2023,64(3):34.

[7] Pinto-Fraga J, López-Miguel A, González-García MJ, et al. Topical fluorometholone protects the ocular surface of dry eye patients from desiccating stress: a randomized controlled clinical trial. Ophthalmology, 2016,123(1):141-153.

[8] Liu SH, Saldanha IJ, Abraham AG, et al. Topical corticosteroids for dry eye. Cochrane Database Syst Rev, 2022,2022(10):CD015070.

[9] Donnenfeld E, Pflugfelder SC. Topical ophthalmic cyclosporine: pharmacology and clinical uses. Surv Ophthalmol, 2009, 54(3): 321-338.

[10] Locatelli EVT, Acuna KA, Betz J, et al. Comparison of subjective responses to cyclosporine 0.05% versus lifitegrast 5.0% in individuals with dry eye disease. Cornea, 2024,43(1):88-94.

[11] Assi L, Lutfallah SC, Yim TW, et al. Topical lifitegrast therapy for dry eye disease. Cochrane Database Syst Rev, 2025,6(6):CD016117.

[12] Tauber J, Laurie GW, Parsons EC, et al. Lacripep for the treatment of primary sjögren-associated ocular surface disease: results of the first-in-human study. Cornea, 2023,42(7):847-857.

[13] Li J, Xuan ZY, Liu CN. Long non-coding RNAs and complex human diseases. Int J Mol Sci, 2013,14(9):18790-18808.

[14] Yang YH, Chen MJ, Zhai ZM, et al. Long non-coding RNAs Gabarapl2 and Chrnb2 positively regulate inflammatory signaling in a mouse model of dry eye. Front Med, 2021,8:808940.

[15] Zhang ZZ, Zhang LW, Chen BH. Characterization of T cells in the progression of dry eye disease using single-cell RNA sequencing in mice. Eur J Med Res, 2025,30(1):338.

[16] Kim D, Langmead B, Salzberg SL. HISAT: a fast spliced aligner with low memory requirements. Nat Methods, 2015,12(4):357-360.

[17] Trapnell C, Williams BA, Pertea G, et al. Transcript assembly and quantification by RNA-Seq reveals unannotated transcripts and isoform switching during cell differentiation. Nat Biotechnol, 2010, 28(5): 511-515.

[18] Love MI, Huber W, Anders S. Moderated estimation of fold change and dispersion for RNA-seq data with DESeq2. Genome Biol, 2014, 15(12):550.

[19] Kovaka S, Zimin AV, Pertea GM, et al. Transcriptome assembly from long-read RNA-seq alignments with StringTie2. Genome Biol, 2019,20(1):278.

[20] Kong L, Zhang Y, Ye ZQ, et al. CPC: assess the protein-coding potential of transcripts using sequence features and support vector machine. Nucleic Acids Res, 2007, 35 (Web Server issue): W345-W349.

[21] Wang GY, Yin HY, Li BY, et al. Characterization and identification of long non-coding RNAs based on feature relationship. Bioinformatics, 2019,35(17):2949-2956.

[22] Sun L, Luo HT, Bu DC, et al. Utilizing sequence intrinsic composition to classify protein-coding and long non-coding transcripts. Nucleic Acids Res, 2013,41(17):e166.

[23] Wang LG, Park HJ, Dasari S, et al. CPAT: Coding-Potential Assessment Tool using an alignment-free logistic regression model. Nucleic Acids Res, 2013,41(6):e74.

[24] Yang RC, Huang F, Fu JY, et al. Differential transcription profiles of long non-coding RNAs in primary human brain microvascular endothelial cells in response to meningitic *Escherichia coli*. Sci Rep, 2016,6:38903.

[25] Xie C, Mao XZ, Huang JJ, et al. KOBAS 2.0: a web server for annotation and identification of enriched pathways and diseases. Nucleic Acids Res, 2011,39(suppl_2):W316-W322.

[26] Iyer MK, Niknafs YS, Malik R, et al. The landscape of long noncoding RNAs in the human transcriptome. Nat Genet, 2015,47(3): 199-208.

[27] Zhang LX, Dong YH, Wang YJ, et al. Long non-coding RNAs in ocular diseases: new and potential therapeutic targets. FEBS J, 2019, 286(12):2261-2272.

[28] Du M, Yuan L, Tan X, et al. The LPS-inducible lncRNA Mirt2 is a negative regulator of inflammation. Nat Commun, 2017,8(1):2049.

[29] Danga AK, Rath PC. Cellular and molecular functions of long noncoding RNAs in testis, aging and diseases. Biogerontology, 2025, 26(5):166.

[30] Statello L, Guo CJ, Chen LL, et al. Gene regulation by long non-coding RNAs and its biological functions. Nat Rev Mol Cell Biol, 2021, 22(2):96-118.

[31] Zuo X, Zeng H, Wang BW, et al. AKR1C1 protects corneal epithelial cells against oxidative stress-mediated ferroptosis in dry eye. Invest Ophthalmol Vis Sci, 2022,63(10):3.

[32] Pucker AD, Ngo W, Postnikoff CK, et al. Tear film miRNAs and their association with human dry eye disease. Curr Eye Res, 2022, 47(11):1479-1487.

[33] Huang W, Tourmouzis K, Perry H, et al. Animal models of dry eye disease: useful, varied and evolving (Review). Exp Ther Med, 2021,22(6):1394.

[34] Wu YQ, Ye H, Zhang H, et al. Characterizing inflammatory, nerve innervation, and immune alterations in three dry eye disease animal models. Exp Eye Res, 2025,260:110580.

[35] Liang LH, Yang X, Zeng H, et al. S100A9-TLR4 axis aggravates dry eye through the blockage of autophagy. Exp Eye Res, 2024, 247: 110052.

[36] Gallowitsch-Puerta M, Pavlov VA. Neuro-immune interactions *via* the cholinergic anti-inflammatory pathway. Life Sci, 2007,80(24-25): 2325-2329.

[37] Alam J, Yaman E, de Paiva CS, et al. Changes in conjunctival mononuclear phagocytes and suppressive activity of regulatory macrophages in desiccation induced dry eye. Ocul Surf, 2024, 34: 348-362.

[38] Alam J, Yaman E, Silva GCV, et al. Single cell analysis of short-

term dry eye induced changes in cornea immune cell populations. Front Med (Lausanne), 2024,11:1362336.
[39] Wang WH, Wu HY, Xue JW, et al. Intermittent fasting ameliorates diabetes-induced meibomian gland dysfunction in mice. Int J Ophthalmol, 2026,19(5):846-857.
[40] Huang RR, Zhang Y, Han B, et al. Circular RNA HIPK2 regulates astrocyte activation *via* cooperation of autophagy and ER stress by targeting MIR124-2HG. Autophagy, 2017,13(10):1722-1741.
[41] Choi W, Li ZR, Oh HJ, et al. Expression of CCR5 and its ligands CCL3,-4, and-5 in the tear film and ocular surface of patients with dry eye disease. Curr Eye Res, 2012,37(1):12-17.
[42] Malesiński R, Bakunowicz-Łazarczyk A, Wysocka J. The role of chemokines CCL3/MIP-1 Alfa and CCL4/MIP-1 beta in pathogenesis of dry eye syndrome. Klin Oczna, 2008,110(7-9):277-279.
[43] Enriquez-de-Salamanca A, Castellanos E, Stern ME, et al. Tear cytokine and chemokine analysis and clinical correlations in evaporative-type dry eye disease.Mol Vis, 2010,16:862-873.
[44] Baratta RO, Schlumpf E, Buono BJD, et al. Corneal collagen as a potential therapeutic target in dry eye disease. Surv Ophthalmol, 2022, 67(1):60-67.
[45] Ng A, Xavier RJ. Leucine-rich repeat (LRR) proteins: integrators of pattern recognition and signaling in immunity. Autophagy, 2011,7(9):1082-1084.
[46] Lin X, Liu YW, Li JN, et al. Depression induces ocular surface inflammation and dry eye-like changes in mice. Int J Ophthalmol, 2026, 19(3):434-442.
[47] Cha MJ, Cho H, Yeon Y, et al. Protective effects of miR-16-5p and miR-142-3p on inflammation and autophagy in human corneal epithelial cells under hyperosmotic stress *in vitro*. Int J Mol Sci, 2025, 27(1):422.
[48] Xu B, Ji XN, Li LF, et al. miR-93-5p loaded lipid nanoparticles break the dry eye vicious cycle *via* targeting MAP3K8. ACS Appl Mater Interfaces, 2026,18(13):18740-18754.
[49] Liu S, Yang G, Li QN, et al. Abnormal expression of lncRNA SNHG7 in dry eye disease and its effect on human conjunctival epithelial cells. Tohoku J Exp Med, 2025,266(2):185-191.